# Transmit and Receive of a cMUT Cell: Modeling and Experiments

S.P. Mao[1,2,*], X. Rottenberg[1], V. Rochus[1], P. Helin[1], A. Verbist[1], S. Severi[1], B. Nauwelaers[2] and H.A.C. Tilmans[1]

[1] imec v.z.w., Kapeldreef 75, B-3001 Leuven, Belgium
[2] Department of Electronic Engineering, Katholieke Universiteit Leuven, Leuven, Belgium
[*]Corresponding author: mao@imec.be

## ABSTRACT

This paper presents the equivalent circuit modeling and experimental verification of the transmit and receive properties of a single cell capacitive micromachined ultrasonic transducer (cMUT). A key achievement of this paper is a confirmation that the equivalent circuit model, presented in one of our previous publications, provides a sound model. The results predicted by the model are in rather good agreement with experimental results, and this for a single cMUT cell operated in both transmit and receive mode. The equivalent circuit model thus provides an easy way to rapidly predict the behavior of cMUT cells of arbitrary shape. The model can further be adapted and used to study a family of cells as in elements or arrays.

***Keyword***s: cMUT, transmit, receive, equivalent circuit modeling, experimental verification

## 1. INTRODUCTION

Capacitive micromachined ultrasonic transducers (cMUTs) are recognized as key enablers for many promising applications such as medical imaging and therapy, chemical or bio-sensing, acoustic manipulation, obstacle detection, acoustic telecommunication [1],[2]. cMUTs are used in arrays. In order to predict the behaviors of large arrays, the key step is the modeling and its corresponding validation of a single cMUT cell. As a result, a fast and precise way to predict both the transmit and receive characteristics of cMUTs is preferred. Analytical model based on equivalent circuit modeling has been widely used for the simulation of cMUTs [3-5]. Most of these models are based on the static deflection of the cMUT membrane thus only a low frequency approximation. A modal analysis based analytical equivalent circuit model was introduced in one of our previous publications [6]; though only the fundamental mode branch was described there, harmonic mode branches can be added in a similar way [7]. Our model allows simulation of the dynamic characteristics of a cMUT cell for a very wide frequency range not limited to the vicinity of the fundamental mode.

In this paper, we present a comparison of the results from the equivalent circuit modeling and experiments of cMUT cells. The cMUT cells fabricated by imec's SiGeMEMS-based technology are used as a test vehicle (Fig. 1) [8]. Both the transmit and receive characteristics of a cMUT cell have been examined, and good agreements between modeling and experiments are reached.

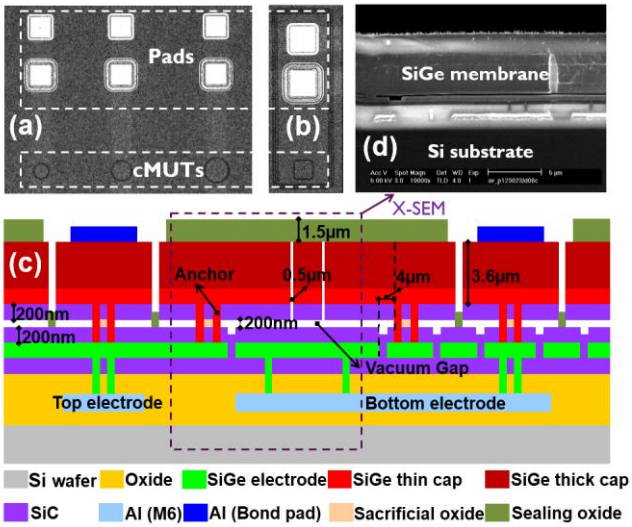


Figure 1: Devices: (a) Micrographs of the circular cMUT cells; (b) Micrographs of the square cMUT cell; (c) Schematic of the cross-sectional view of a cMUT cell; (d) X-SEM of a local cross-section of a cMUT cell.

## 2. MODELING AND EXPERIMENTS

### 2.1. Equivalent Circuit Model

The equivalent circuit model of a circular cMUT cell has already been explained in one of our previous publications [6]. It is presented in Fig. 2, using the same component definition as in [6], with the additional equivalent circuit of the receive set-up. $L_c$ and $C_c$ denote the internal impedance of the coaxial cable which transports the receive signal to the oscilloscope, $C_s$ and $R_s$ are the oscilloscope impedance, and details are shown in the experiment session. However, some slight modifications are needed in this model to match the realistic cases. The mechanical stiffness $k_1$ should be adjusted to include the effect of the cMUT anchor or the squeeze air damping, in order to make this modified analytical natural frequency match the experimental results. In addition, the piston radiation impedance approximation is not accurate enough to represent the radiation impedance of the flexural mode of the cMUT membrane. The clamped circular membrane radiation impedance derived by Porter is used for the equivalent circuit [9].

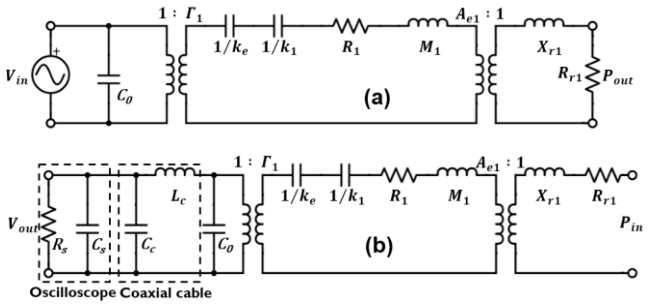


Figure 2: Equivalent circuit of a cMUT cell: (a) Transmit; (b) Receive. (Illustration by the first mode branch)

## 2.2. Experiments

The transmit characterization of the cMUT cell is based on the cMUT test platform presented in [10] (Fig. 3(a)). The cMUT cell is immersed in Fluorinert (FC-84, 3M, USA) and driven by either a pulse or a sine wave burst superimposed on a (high) DC voltage bias. A needle type calibrated hydrophone (HNP1000, Onda Inc., USA) is used to detect the sound pressure at a certain distance from the transducer surface.

Receive measurements are performed on the same test platform as used for the transmit measurements (Fig. 3(b)). A calibrated PVDF transducer (PA363, Precision Acoustics, UK) is used to generate the ultrasound wave. The transducer is placed at a fixed distance 11mm from the cMUT chip. It can be actuated either by a sine wave burst or a short (50ns) pulse. Thus it generates an input pressure on the cMUT device. The cMUT device is biased by a (high) DC voltage at one pad. The other pad, DC grounded, connected to an oscilloscope through a coaxial cable. The oscilloscope has an input impedance of a 1MΩ resistance parallel with a 13pF capacitance. The coaxial cable has a 105pF capacitance and a 1.2e-6H inductance, they are both measured values.

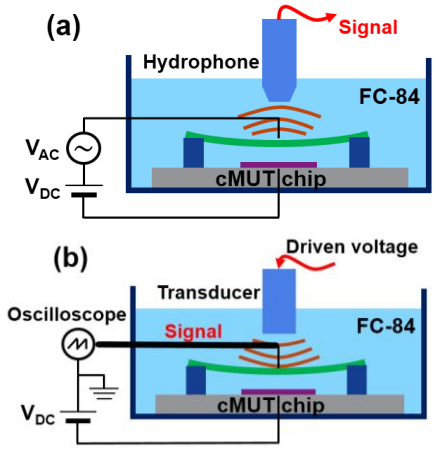


Figure 3: Schematic of the experimental set-ups: (a) Transmit; (b) Receive.

# 3. RESULTS AND DISCUSSION

## 3.1. Transmit

The transmit test is performed on the three circular cMUT cells shown in Fig. 1(a). These devices have the same dielectric gap composition (400nm SiC/200nm vacuum gap/400nm SiC). Their geometries and driven conditions are listed in Table 1. They are biased by a DC voltage which is around 70% of the theoretical pull-in voltage, and the applied 50ns width pulse voltage is around 10% of the theoretical pull-in voltage for the pulse response experiments. A sine wave burst superimposed on the DC voltage is used for the evaluation of the output pressure amplitude of cMUT cells at a certain frequency.

Axial pressure amplitude comparisons are shown in Fig. 4 based on the three circular cMUT cells. The methodology similar to that described in [10] is used to calculate the spatial pressure field by the transducer surface velocity from the equivalent circuit model. A transition from near field to far field of the hydrophone is found around 3mm distance by the hydrophone measurement results. It also means only the measurement results farther than that distance are to be trusted. Therefore, the simulation and measurement results relevantly match in the far field region of cMUTs.

Table 1: Geometries and driven conditions of these devices.

| | Device I | Device II | Device III |
|---|---|---|---|
| Diameter [μm] | 60 | 80 | 100 |
| DC voltage [V] | 350 | 200 | 150 |
| Pulse voltage [V] | 50 | 30 | 20 |
| Sine wave burst | 20 cycles, 17$V_{pp}$, 6MHz | | |

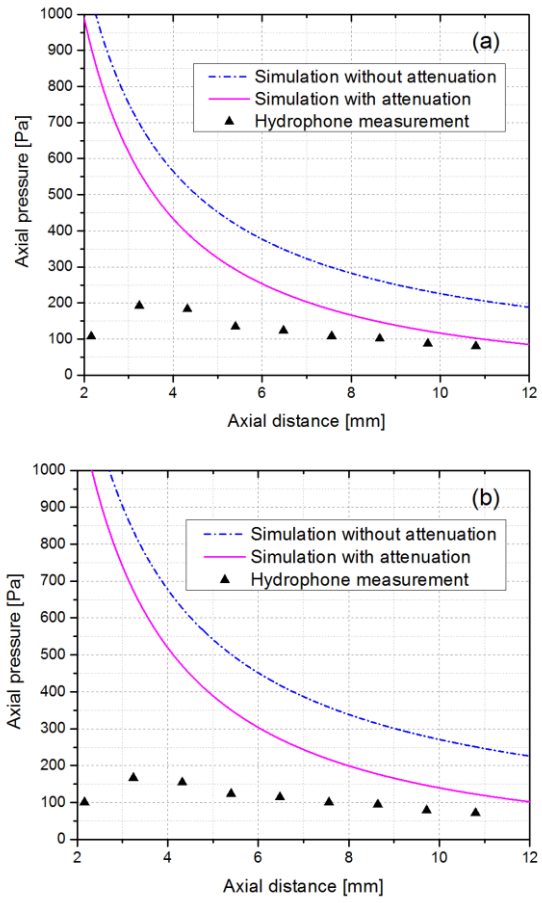

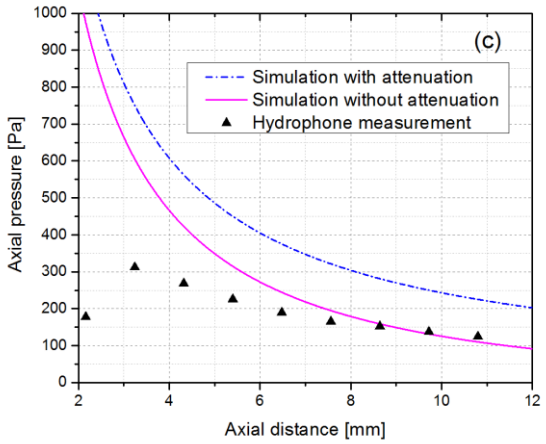


Figure 4: Axial pressure amplitude of the three cMUT cells: (a) Device I; (b) Device II; (c) Device III.

Figure 5 shows the pulse response spectrum of the three cMUT cells. Hydrophone measurements are done at 4.4mm distance from the cMUT. A 2μs width Hanning window is applied on the detected signal to lower the noise, and the whole signal duration is 8μs. The dash dot blue line is the measurement result. The magenta line is the measurement result corrected to the hydrophone sensitivity, the fluid attenuation and the diffraction compensation [10]. Results are all normalized to the maximum pressure. All of the three figures show good matches for the center frequency between modeling and experiment. The shape differences of the pulse response becomes significant in Fig. 5(c), which corresponds to the 100μm diameter cell. There are at least two reasons for the increased mismatch. On the one hand, the frequency range is already far away from the fundamental frequency, and the model is only an approximation when the frequency range is close to it. On the other hand, the harmonic modes cannot be neglected. The second peak around 8MHz is corresponding to the frequency range of the first axisymmetric harmonic mode. It also means more than one mode branch in the equivalent circuit is needed in order to simulate a wide frequency band.

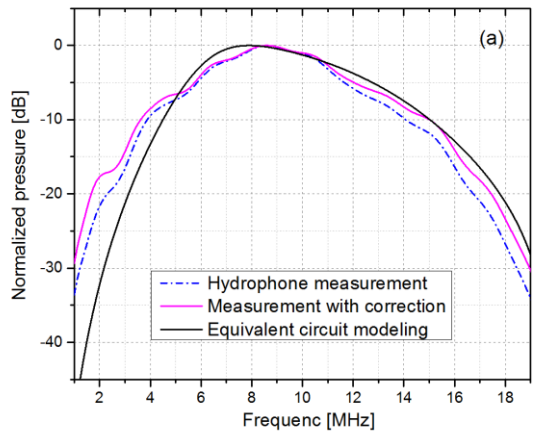


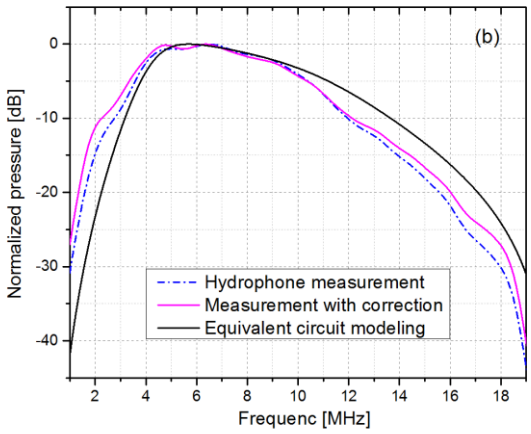


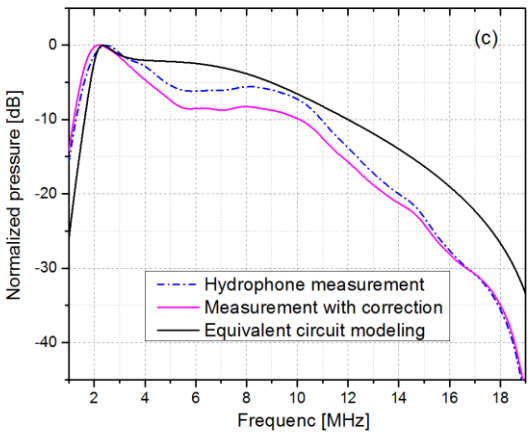


Figure 5: Pulse response spectrum of the three cMUT cells: (a) Device I; (b) Device II; (c) Device III.

## 3.2. Receive

A 60μm side-length square cMUT cell with three different types of dielectric gaps is used for the receive (Fig. 1(b)): Gap type I (400nm SiC/200nm vacuum gap/400nm SiC), Gap type II (200nm SiC/200nm vacuum gap/200nm SiC), and Gap type III (200nm SiC/158nm vacuum gap/200nm SiC). The transducer is driven by a 75 cycle 6 MHz sine wave burst, and an corresponding 2.8kPa input pressure is applied on the cMUT chip. Two types of comparison are performed; one comparison is with the same DC bias (100V) but with the three types of gaps, and the other comparison is based on the Gap type II with different DC biases. Results are shown in Fig. 6, a good agreement is obtained between measurement and modeling. Those small mismatches are attributed to the experimental errors such as the calibration of the transducer, misalignment of the source and the cMUT cell. The highest measured receive sensitivity is obtained on the Gap type III device with a value of 0.0125 mV/kPa. However this value can be affected by the DC bias voltage, the coaxial cable properties and the oscilloscope impedance.

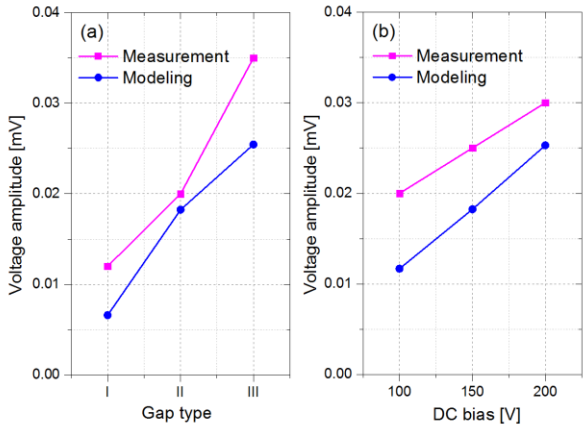


Figure 6: The receive signal amplitude of the square cMUT cells: (a) Gap effect based on three Gap type cMUT cells (DC bias 100V); (b) Bias effect based on the Gap type II cMUT cell.

Receive frequency response of the square cMUT cell is also done by the same transducer, which is driven by a 50ns duration 80V pulse. A very wide bandwidth pressure (the center frequency is around 6MHz, the -3dB fractional bandwidth is larger than 100%) is applied on the cMUT cell. Therefore, in the interested frequency region, a constant pressure input can be used as an approximation in the frequency sweep simulation of the equivalent circuit. The cMUT cells are biased by a DC voltage (Gap type I: 100V, Gap type II: 150V, and Gap type III: 200V), and the different bias conditions are for clear response signals. The 2μs width Hanning window is used, and the frequency spectrum of the measured receive signal is shown in Fig. 7(a). Fluctuations are found since the very low signal-noise-ratio (SNR) and make the actual signal difficult to recognize. However, if we compare the measurement results with the results from the equivalent circuit (Fig. 7(b)), they show the similar behaviors. Further work is still needed to draw a stronger conclusions.

## CONCLUSIONS

This paper studies the correlation between the equivalent circuit modeling and experimental characterizations based on a single cMUT cell. Both the transmit and receive comparisons are performed on the single cMUT cell with two kinds of shapes and different dimensions. Good agreements are obtained on both amplitude and frequency response. It proves our model is a fast and effective tool to predict the behaviors of the cMUT cells for both transmit and receive. The similar methodology can be used to study the behaviors of large cMUT arrays, the model of which is already beyond the practical limitation of the FEM simulation.

## ACKNOWLEDGE

The authors should thank Dr. Piotr Czarnecki and Dr. Jeroen De Coster for the help during the cMUT test.

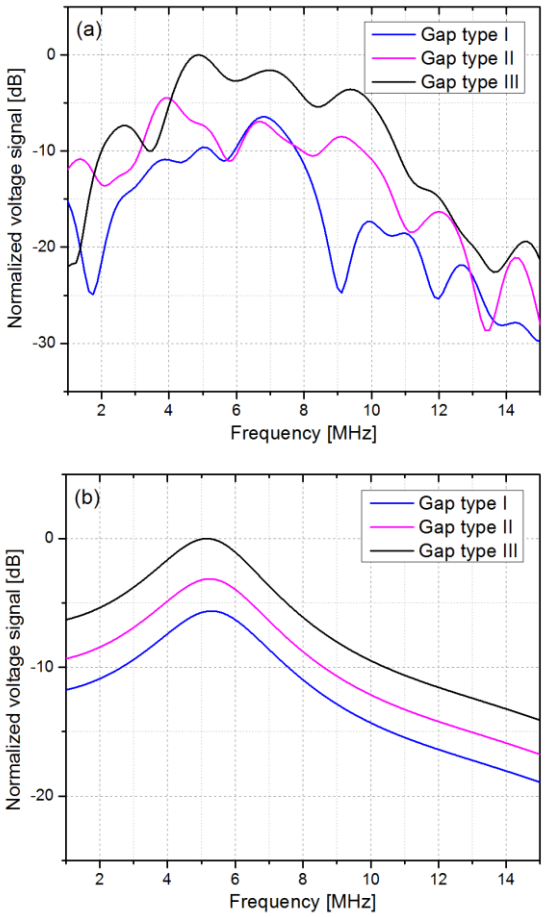


Figure 7: Receive frequency responses of the square cMUT cells: (a) Measurement; (b) Modeling.

## REFERENCES

[1] B. T. Khuri-Yakub and O. Oralkan, J. Micromech. Microeng., 21, 054004(11pp), 2011.
[2] K. K. Park, etc., Sensor. Actuat. B-Chem., 160, 1120-1127, 2011.
[3] I. O. Wygant, M. Kupnik, and B. T. Khuri Yakub, Proc. IEEE Ultrason. Symp., 2111-2114, 2008.
[4] A. Caronti, G. Caliano, A. Iula, and M. Pappalardo, IEEE Trans. Ultrason. Ferroelectr. Freq. Control., 49, 159-168, 2002.
[5] A. Lohfink and P. C. Eccardt, IEEE Trans. Ultrason. Ferroelectr. Freq. Control., 52, 2163-2172, 2005.
[6] X. Rottenberg, A. Erismis, P. Czarnecki, Ph. Helin, A. Verbist and H. A. C. Tilmans, EuroSimE 2012, 1-6, 2012.
[7] H.A.C. Tilmans, J. Micromech. Microeng., 6, 157-176, 1996.
[8] Ph. Helin, P. Czarnecki, A. Verbist, G. Bryce, X. Rottenberg, and S. Severi, Proc. of MEMS, 305-308, 2012.
[9] D. T. Porter, J. Acoust. Soc. Am., 36, 1154-1161, 1964.
[10] S.P. Mao, X. Rottenberg, V. Rochus, B. Nauwelaers and H.A.C. Tilmans, EuroSimE 2014, accepted.